JOURNAL OF MATERIALS SCIENCE 15 (1980) 2448–2454

Deformation of single crystals of the $L2_1$ ordered Ag_2MgZn

MASAHARU YAMAGUCHI,* YUKICHI UMAKOSHI
Department of Materials Science and Engineering, Osaka University, Yamada-kami, Suita, Osaka 565, Japan

The orientation and temperature dependence of slip geometry and yield stress in single crystals of the $L2_1$ ordered Ag_2MgZn has been studied in compression in the temperature range 290 to 580 K. The slip direction in Ag_2MgZn is exclusively $\langle 1\,1\,1 \rangle$ in this temperature range, but the slip plane varies with crystal orientations; slip occurs on $(\bar{2}\,1\,1)$ for orientations near the $[0\,1\,1]$–$[\bar{1}\,1\,1]$ boundary, while for the other orientations in the $[0\,0\,1]$–$[0\,1\,1]$–$[\bar{1}\,1\,1]$ unit triangle it occurs on the $(\bar{1}\,0\,1)$. The critical resolved shear stress (CRSS) for slip on both the $(\bar{1}\,0\,1)$ $[1\,1\,1]$ and $(\bar{2}\,1\,1)$ $[1\,1\,1]$ systems increases abnormally with increasing temperature and reaches a maximum peak at about 0.92 of the critical temperature T_c, for the $L2_1$-type order. The peak temperature and the shape of the CRSS versus temperature curve are independent not only of crystal orientation but also of the operative slip system. It is suggested that the strength anomaly in Ag_2MgZn be interpreted in terms of the mechanism based on the transition from unit dislocations to superdislocations.

1. Introduction

The anomalous peak in flow stress occurring in ordered alloys at some intermediate temperature has been the subject of many investigations [1–3]. However, most of the investigations of this anomalous flow stress behaviour have been carried out on ordered alloys with the $L1_2$-type superlattices and comparatively little has been done on ordered alloys having bcc-based superlattices such as B2, DO_3 and $L2_1$. Of the alloys exhibiting these ordered lattices, only β brass (B2) [4–10], FeCo (B2) [11–13] and Fe_3Al (DO_3) [14, 15] have been studied with respect to this anomalous flow stress behaviour. To make meaningful comparisons and then obtain a general understanding concerning the flow stress anomaly in ordered alloys with bcc-based superlattices, a reasonable number of these alloys should be studied with respect to this anomaly.

To our knowledge, no such investigations have been done on $L2_1$ ordered alloys. It was, therefore, decided to examine the mechanical properties of the $L2_1$ ordered Ag_2MgZn in some detail. Ag_2MgZn was chosen because it has the relatively low critical temperature of $T_c = 523$ K for the $L2_1$-type order [16] and its single crystals can be prepared easily the Bridgman method.

In this paper, experimental results are reported on the temperature and orientation dependence of slip geometry and yield stress in Ag_2MgZn single crystals in the range 290 to 580 K.

2. Experimental procedure

The alloys were prepared by melting together accurately weighed amounts of high purity silver (99.99%), zinc (99.999%) and magnesium (99.9%) to give the Ag_2MgZn composition. The components were first cut into small pieces, thoroughly mixed, mounted on a graphite crucible and then melted together under an argon atmosphere in a sealed silica tube. The crystals were grown from the alloys by the Bridgman method and homogenized

*Present address: Department of Metallurgy and Materials Science K1, University of Pennsylvania, Philadelphia, PA 19104, USA.

 0022–2461/80/102448–07 $02.70/0

at 870 K for 48 h. Orientated specimens of approximately 3 mm x 3 mm cross section and 7 mm length were cut from the homogenized crystals by spark machining and subsequently chemically polished in a solution of CrO_3 (50 g), HCl (5 cm^3) and water (500 cm^3) to remove the surface damage. The specimens were annealed at 870 K for 2.5 h and then slowly cooled at 8.3 $K h^{-1}$ to room temperature. All the specimens were repolished prior to testing.

Compression tests were conducted on an Instron type machine at a nominal strain rate of $2.4 \times 10^{-4}\,sec^{-1}$ in the temperature range 290 to 580 K. Specimens were deformed to about 1% compression strain and slip traces were examined with an optical microscope using Nomarski interference contrast. Operative slip systems were determined by the two-surface trace analysis method. The term "top face" used in this paper means the surface that is approximately normal to the surface containing the primary Burgers vector and compression axis. The stress axis is referred to the standard [0 0 1]–[0 1 1]–[$\bar{1}$ 1 1] unit triangle.

Specimens for X-ray diffraction analysis were filed and annealed in a similar way to that used for compression specimens.

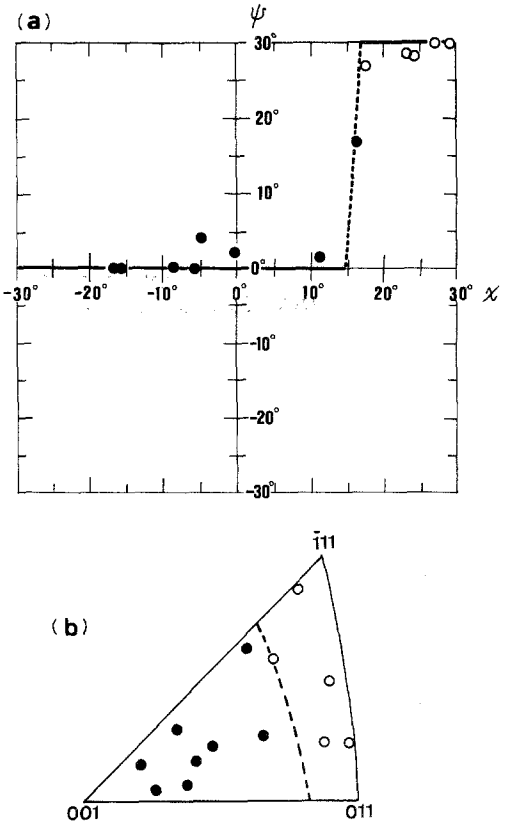

Figure 1 The observed slip plane variation with crystal orientation: (a) $\psi - \chi$ curve; (b) orientations of crystals.

3. Experimental results

3.1. X-ray diffraction analysis

Crystal structure of the annealed sample was examined by the X-ray diffractometer, at room temperature, with Cu$K\alpha$ radiation. The alloy was found to be in an ordered state, with a structure of the $L2_1$-type. The lattice parameter was 6.464 Å in a $L2_1$-type unit cell, which is about the same as that reported for stoichiometric Ag_2MgZn [16].

3.2. Observed slip systems

Optical microscopy of slip traces on crystals with various orientations revealed that the slip direction in the Ag_2MgZn was exclusively ⟨1 1 1⟩, but the slip plane varied with the orientation of crystal, similar to the behaviour in single crystals of bcc metals and alloys, see the review by Christian [17]. Fig. 1a, for example, shows the slip plane variation with orientation at 470 K, where observed slip planes for various orientations (Fig. 1b) are plotted in the form of conventional $\psi - \chi$ relation for bcc metals. χ is the angle between the maximum resolved shear stress plane in the [1 1 1] zone and ($\bar{1}$ 0 1), and ψ is the angle between the observed slip plane and ($\bar{1}$ 0 1). It is seen from the figure that for orientations near the [0 1 1]–[$\bar{1}$ 1 1] boundary slip occurs on ($\bar{2}$ 1 1), while for the other orientations it takes place on ($\bar{1}$ 0 1). The broken line boundary in the unit triangle will be discussed later. The $\psi - \chi$ relationship for this compound in the temperature range 290 to 500 K was almost the same as that shown in Fig. 1b. Above 500 K, however, slip traces became increasingly wavy, so that it was not always possible to determine slip planes clearly.

Slip lines corresponding to slip on the ($\bar{1}$ 0 1) and ($\bar{2}$ 1 1) planes are shown in Figs. 2a to d, which were observed on the top faces of crystals deformed at 290 and 480 K. Slip lines for the ($\bar{2}$ 1 1) slip are generally finer and more homogeneous than those for the ($\bar{1}$ 0 1) slip, and as the deformation temperature is decreased, this difference in slip line character becomes more apparent. It was also interesting that even when the orientation of crystal was such that the primary slip occured on the ($\bar{2}$ 1 1) plane, continued straining of the crystal produced additional very coarse slip bands corresponding to slip on the ($\bar{1}$ 0 1) plane. Fig. 3

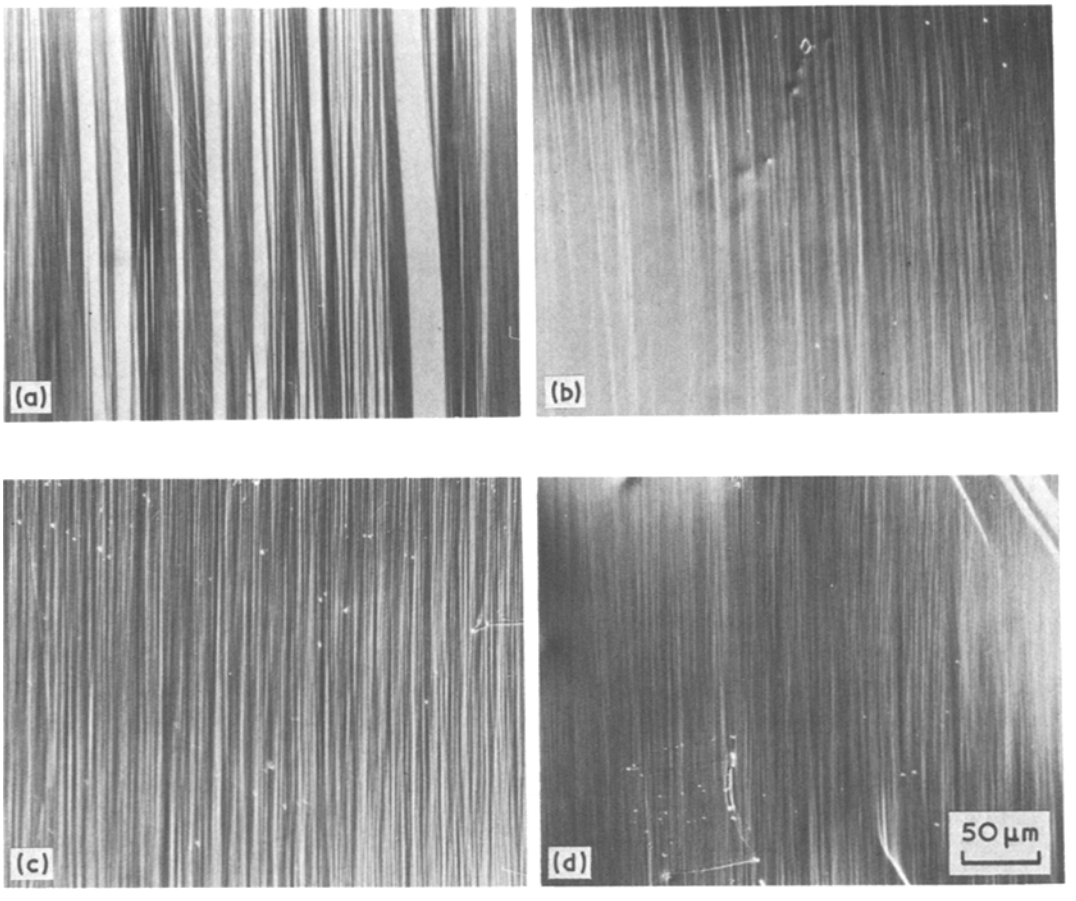

Figure 2 Slip lines on the top face of crystals deformed at 290 and 480 K: (a) $(\bar{1}\,0\,1)$ slip at 290 K; (b) $(\bar{1}\,0\,1)$ slip at 480 K; (c) $(\bar{2}\,1\,1)$ slip at 290 K; (d) $(\bar{2}\,1\,1)$ slip at 480 K.

shows such coarse slip bands observed on the top face of a crystal with $\chi = 27^\circ$ and deformed at 393 K. The occurrence of such an additional coarse slip on $(\bar{1}\,0\,1)$ was, however, limited to the temperature range below about 500 K.

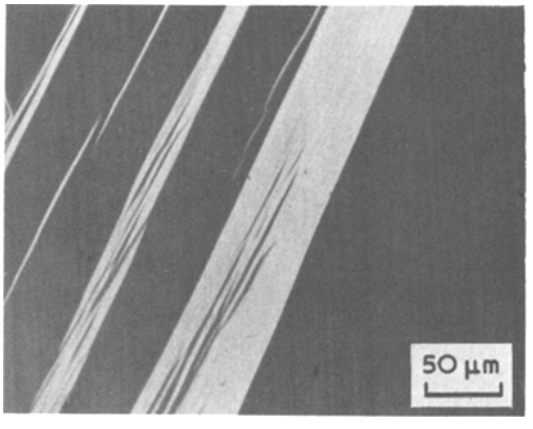

Figure 3 Coarse slip bands on the top face of a crystal with $\chi = 27^\circ$ deformed at 393 K.

3.3. Temperature dependence of yield stress

The critical resolved shear stress (CRSS) for slip on the $(\bar{2}\,1\,1)$ [1 1 1] and $(\bar{1}\,0\,1)$ [1 1 1] systems calculated using the 0.2% offset yield stress is plotted in Figs. 4a and b against temperature in the range 290 to 580 K. Although slip planes are not very clear above 500 K, CRSS for each of the two slip systems in this temperature range have been calculated assuming that the slip plane above 500 K is the same as that below 500 K. Even so, it is clearly seen from the figures that an anomalous peak occurs in this material. The CRSS for slip on both systems begins to increase gradually at 350 K and reaches a maximum peak around 480 K which is about $0.92\,T_c$, and then decreases rapidly with increasing temperature. It should be noted that not only the peak temperature but also the shape of the CRSS versus temperature curve are practically the same for slip on both systems, although the CRSS for slip on the $(\bar{2}\,1\,1)$ plane is between 2 and

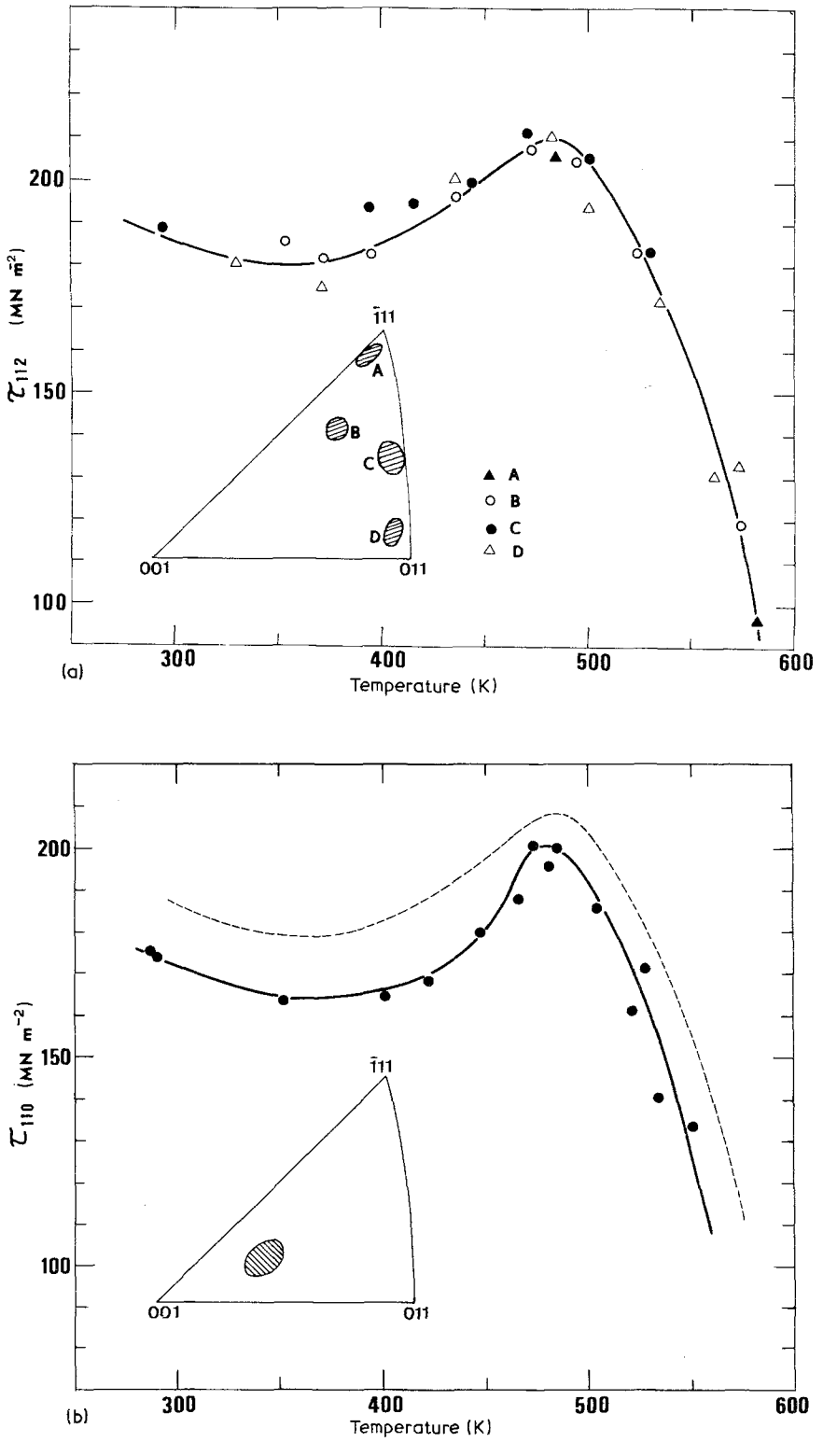

Figure 4 The temperature dependence of critical resolved shear stress in Ag_2MgZn single crystals; (a) CRSS for the $(\bar{2}\,1\,1)$ [1 1 1] slip; (b) CRSS for the $(\bar{1}\,0\,1)$ [1 1 1] slip (solid line) and the $(\bar{2}\,1\,1)$ [1 1 1] slip (broken line) for comparison.

10% higher than that for the $(\bar{1}\,0\,1)$ slip. As seen in Fig. 4a, the CRSS for the $(\bar{2}\,1\,1)$ plane was obtained for four different orientations. Although some scatter in the results is evident, the CRSS seems to be independent of orientation. Such a marked CRSS law violation as that observed in some $L1_2$ alloys [18–22] and β brass [8] is not seen in the case of Ag_2MgZn.

The regions of orientations where the two observed slip systems should be operative at 470 K were calculated using the values of the CRSS for the two slip systems shown in the figure. The calculated boundary is shown by the broken line in Fig. 1b. The observed slip systems are found to be in agreement with the calculations.

4. Discussion

4.1. Configuration of superdislocations and operative slip systems

It has been generally known that the operative slip planes and the nature of slip surfaces in ordered alloys with bcc-based superlattices are sensitive to the separation of superpartial dislocations. In $L2_1$ ordered alloys with $\langle 1\,1\,1\rangle$ slip vector, superdislocations are usually composed of four superpartials with Burgers vectors $a_0/2\langle 1\,1\,1\rangle$ referred to the disordered bcc unit cell [23]. They are separated by two types of antiphase boundaries, that is, APBI having APB energy γ_I and APBII having the energy γ_{II}, as shown in Fig. 5. The equilibrium separations r and r_1 can be estimated using the following equations [23, 24]

$$\frac{2}{(r-r_1)}+\frac{1}{r}+\frac{1}{(r-2r_1)}=\frac{\gamma_{II}}{A(\theta)}, \quad (1)$$

$$\frac{1}{r_1}-\frac{1}{(r-r_1)}-\frac{1}{(r-2r_1)}=\frac{\gamma_I-\gamma_{II}}{A(\theta)} \quad (2)$$

and

$$A(\theta)=\frac{Gb^2}{2\pi}\left[\sin^2\theta+\frac{\cos^2\theta}{(1-\nu)}\right], \quad (3)$$

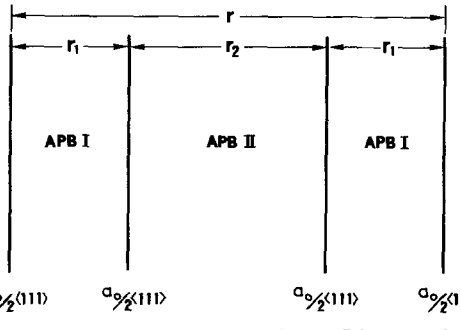

Figure 5 Superlattice dislocation in an $L2_1$ superlattice [23].

where G is the shear modulus, $\boldsymbol{b}=a_0/2\langle 1\,1\,1\rangle$ is the Burgers vector of each superpartial, ν is Poisson's ratio and θ is the angle between the Burgers vector and the dislocation line direction. APBII involves a net change of only second nearest neighbour bonds and therefore for the case of stoichiometric A_2BC composition γ_{II} for any plane $\{h\,k\,l\}$ can be simply given by the following well known equation [23, 25]

$$\gamma_{II}=\frac{W}{2a_0^2}\frac{h+k+l}{N}, \quad N=h^2+k^2+l^2, \quad (4)$$

where $W=W_{BB}+W_{CC}-2W_{BC}$ is one of the second nearest neighbour ordering energies and W_{BB}, W_{CC} and W_{BC} are the second nearest neighbour interaction energies for B–B, C–C and B–C atom pairs. W has been known to be related to T_c by [26]

$$\tfrac{3}{2}W=kT_c. \quad (5)$$

Thus, γ_{II}, for example, for $\{1\,1\,0\}$ and $\{1\,1\,2\}$ can easily be calculated to be 32.7 and 37.8 mJ m^{-2}, respectively.

On the other hand, APBI involves a complicated change in both first and second nearest neighbour bonds and therefore γ_I cannot be written in a simple form such as Equation 4. Then, in order to see how the separations r and r_1 vary with γ_I, those at room temperature were calculated for various values of γ_I. Fig. 6 shows the results for superdislocations of pure screw and pure edge lying on $\{1\,1\,0\}$ and $\{1\,1\,2\}$. The shear modulus of Ag_2MgZn was estimated by linear interpolation using the shear moduli of AgZn [27] quenched from the β-phase (B2-type) region and AgMg [28]. ν was assumed to be 0.3.

According to the known phase-diagram for AgMg–AgZn quasibinary system [16], Ag_2MgZn possesses B2-type ordered structure at temperatures above T_c and remains ordered in this type up to the melting point. This suggests that this material has considerably large ordering energies associated with first nearest neighbour bonds. Therefore, γ_I is also quite likely to be large and it would not be unrealistic at all to assume that $\gamma_I \geqslant \gamma_{II}$. In fact, in Fe_3Si (DO_3) [29] and Cu_2MnAl ($L2_1$) [30], γ_I has been known to be much higher than γ_{II}. Thus, at room temperature, the separations r and r_1 of superpartials lying on $\{1\,1\,0\}$ are thought to be roughly in the range 95 to 130$\boldsymbol{b}$ and 5 to 35$\boldsymbol{b}$ for screw orientation, and 135 to 180$\boldsymbol{b}$ and 5 to 45$\boldsymbol{b}$ for edge orientation. The separations for $\{1\,1\,2\}$

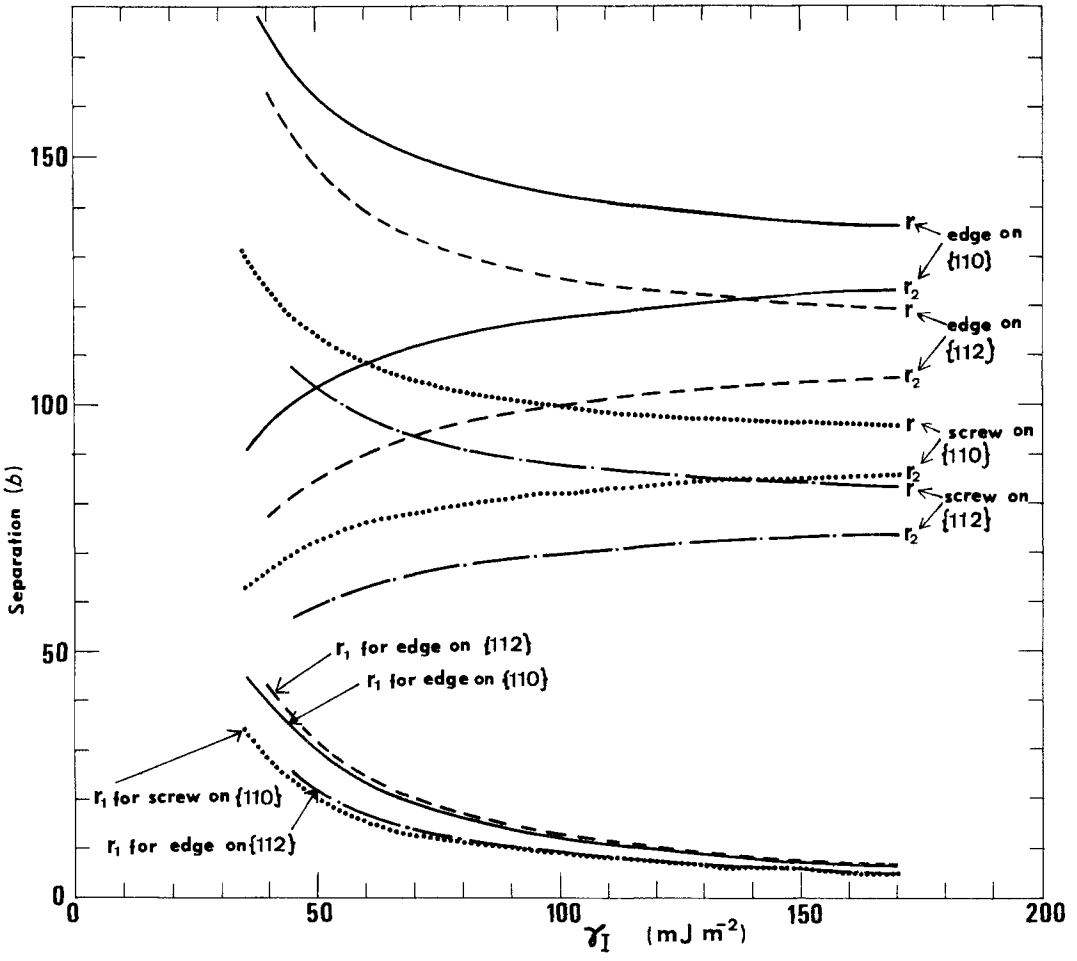

Figure 6 The variation of the separations r, r_1 and r_2 in Fig. 5 with the energy of APBI, γ_I. The separations are given in the unit of b which is the Burgers vector of each superpartial dislocation, $a_0/2\langle 1\,1\,1\rangle$ referred to the disordered bcc unit cell.

are about 10% smaller than those for $\{1\,1\,0\}$. When the separation r is as large as that, the alloy is expected to deform by planar movement of superdislocations confined to the lowest APB energy plane. In the case of FeCo possessing a B2-type structure where superdislocations are composed of two $a_0/2\langle 1\,1\,1\rangle$ superpartials, each superpartial has been thought not to be able to move independently until the separation exceeds about $400b$ [11]. Therefore, it is quite reasonable for slip in Ag_2MgZn single crystals to occur on $\{1\,1\,0\}$, where the APB energies are generally lowest, for most orientations and over a wide range of temperatures. For orientations near the $[0\,1\,1]$–$[\bar{1}\,1\,1]$ boundary, slip was found to occur on $\{1\,1\,2\}$ where the APB energies are generally higher but the reason for this is not clear at present.

4.2. Anomalous strengthening behaviour

The ordered alloys with bcc-based superlattices, β brass [4–10], FeCo [11–13] and Fe_3Al [14, 15] have been known to show the anomaly of an increasing yield strength with increasing temperature. In the present investigation, the anomaly has been found to occur also in Ag_2MgZn. In view of the temperature of the peak in yield strength, Ag_2MgZn is quite similar to FeCo and Fe_3Al but different from β brass; the strength peaks in FeCo, Fe_3Al and Ag_2MgZn occur just below T_c, the critical temperature for ordering of the corresponding ordered structure, while in β brass the peak temperature depends on crystal orientation and is in the range 0.58 to 0.69 T_c [8].

The anomalous strengthening in FeCo and Fe_3Al has been interpreted in terms of the mechanism based on the transition from unit

dislocations to superdislocations [11]. According to the mechanism, the anomalous strength peak occurs at a temperature just below T_c where a large proportion of dislocations begin to move as superdislocations. It is also important that no strong orientation dependence is expected to be observed in the behaviour of the anomalous strengthening due to this mechanism. This is in good agreement with the present observation that the peak temperature and shape of the CRSS versus temperature curve are practically independent not only of crystal orientation but also of the operative slip system. Therefore, the strength anomaly in Ag_2MgZn is likely to be explained by a similar mechanism to that proposed for FeCo and Fe_3Al.

5. Conclusions

(a) Slip in single crystals of the $L2_1$-type ordered Ag_2MgZn occurs on the $(\bar{2}\,1\,1)$ for orientations only near the $[0\,1\,1]$–$[\bar{1}\,1\,1]$ boundary, while it occurs on the $(\bar{1}\,0\,1)$ for the other orientations in the $[0\,0\,1]$–$[0\,1\,1]$–$[\bar{1}\,1\,1]$ unit triangle. The $\{1\,1\,0\}$ slip is likely to be explained by planar movement of superdislocations confined to the lowest APB energy.

(b) CRSS for both the $(\bar{2}\,1\,1)[1\,1\,1]$ and $(\bar{1}\,0\,1)[1\,1\,1]$ slip systems gradually increases with increasing temperature and reaches a maximum peak at around 480 K which is just below T_c. The anomalous strengthening is suggested to be interpreted in terms of the mechanism based on the the transition from unit dislocations to superdislocations.

Acknowledgement

The authors are grateful to Professor T. Yamane for his encouragement.

References

1. N. S. STOLOFF and R. G. DAVIES, *Prog. Mater. Sci.* **13** (1966) 29.
2. L. E. POPOV and N. A. KONEVA in "Order–Disorder Transformations in Alloys" edited by H. Warlimont (Springer-Verlag, Berlin, Heidelberg, New York, 1973) p. 404.
3. S. J. LIANG and D. P. POPE, *Acta Met.* **25** (1977) 485.
4. G. W. ARDLEY and A. H. COTTRELL, *Proc. Roy. Soc.* **219** (1953) 328.
5. N. BROWN, *Phil. Mag.* **4** (1959) 693.
6. K. AOKI and O. IZUMI, *J. Japan Inst. Metals* **36** (1972) 113.
7. M. M. SHEA and N. S. STOLOFF, *Met. Trans.* **5** (1974) 755.
8. Y. UMAKOSHI, M. YAMAGUCHI, Y. NAMBA and K. MURAKAMI, *Acta Met.* **24** (1976) 89.
9. Y. UMAKOSHI and M. YAMAGUCHI, *Scripta Met.* **11** (1977) 211.
10. M. YAMAGUCHI and Y. UMAKOSHI, *Phys. Status Solidi (a)* **43** (1977) 667.
11. N. S. STOLOFF and R. G. DAVIES, *Acta Met.* **12** (1964) 473.
12. P. MOINE, J. P. EYMERY and P. GROSBRAS, *Phys. Status Solidi (b)* **46** (1971) 177.
13. M. J. MARCINKOWSKI in "Order–Disorder Transformations in Alloys" edited by H. Warlimont (Springer-Verlag, Berlin, Heidelberg, New York, 1973) p. 364.
14. A. LAWLEY, E. A. VIDOZ and R. W. CAHN, *Acta Met.* **9** (1961) 287.
15. R. G. DAVIES and N. S. STOLOFF, *ibid.* **11** (1963) 1187.
16. Y. MATSUO, S. MINAMIGAWA and K. KATADA, *ibid.* **25** (1977) 1179.
17. J. W. CHRISTIAN, 2nd International Conference on the Strength of Metals and Alloys, Asilomer 1970 (American Society of Metals, Metals Park, Ohio, 1970).
18. S. M. COPLEY and B. H. KEAR, *Trans. TMS–AIME* **239** (1967) 977.
19. S. TAKEUCHI and E. KURAMOTO, *Acta Met.* **21** (1973) 415.
20. H. PAK, T. SABURI and S. NENNO, *Trans. Japan Inst. Metals* **18** (1977) 617.
21. E. KURAMOTO and D. P. POPE, *Acta Met.* **26** (1978) 207.
22. K. AOKI and O. IZUMI, *J. Mater. Sci.* **13** (1978) 2313.
23. M. J. MARCINKOWSKI and N. BROWN, *Acta Met.* **9** (1961) 764.
24. R. C. RAWFORD, I. L. F. RAY and D. J. COCKAYNE, *Phil. Mag.* **27** (1973) 1.
25. P. A. FLINN, *Trans. TMS–AIME* **218** (1960) 145.
26. Y. MURAKAMI, S. KACHI, N. NAKANISHI and H. TAKEHARA, *Acta Met.* **19** (1971) 97.
27. Y. MATSUO, private communication.
28. J. P. NEUMANN and Y. A. CHANG, *J. Appl. Phys.* **38** (1967) 647.
29. G. E. LAKSO and M. J. MARCINKOWSKI, *Trans. TMS–AIME* **245** (1969) 1111.
30. M. L. GREEN, G. Y. CHIN and J. B. VANDER SANDE, *Met. Trans.* **8a** (1977) 353.

Received 11 December 1979 and accepted 22 February 1980.